

# Design of binocular stereo vision optical system based on a single lens and a single sensor

KUN ZHANG,<sup>1,\*</sup> ZHENG QU,<sup>2,3,4</sup> XING ZHONG,<sup>3</sup> QINGRONG CHEN,<sup>1</sup> AND XI ZHANG<sup>1</sup>

<sup>1</sup>Institute of Optics and Electronics, Chinese Academy of Sciences, Chengdu 610209, China

<sup>2</sup>Changchun Institute of Optics, Fine Mechanics and Physics, Chinese Academy of Sciences, Changchun 130033, China

<sup>3</sup>Chang Guang Satellite Technology Co., Ltd, Changchun 130102, China

<sup>4</sup>e-mail: quzheng16@mails.ucas.ac.cn

\*Corresponding author: zhangkciomp@163.com

Received 18 April 2022; revised 23 June 2022; accepted 13 July 2022; posted 14 July 2022; published 2 August 2022

To reduce the number of detectors used in conventional binocular stereo cameras, while improving the measurement accuracy and compactness of the system, this paper proposes a design method for a binocular stereo vision optical system based on a single lens and a single sensor. First, based on the design principle of the traditional binocular optical system, to the best of our knowledge, a novel method of designing a framing lens array at the optical stop of the optical system is proposed to image two images on one detector simultaneously. Second, we propose a dual-frame lens array design method at the aperture stop position of the optical system that can image two images on one detector simultaneously. Then, the design principle of the method is analyzed theoretically, as well as a detailed analysis of the imaging position layout and the stray light elimination method of the dual-channel optical system. Finally, a single-lens binocular optical system with a focal length of 20 mm and a full field of view of 30° is designed using the method in this paper, and the analysis results demonstrate that the system has the advantages of good imaging quality and compact construction and provides a design idea for the design of a binocular stereo vision optical system. © 2022 Optica Publishing Group

<https://doi.org/10.1364/AO.461564>

## 1. INTRODUCTION

Stereo vision is the process of recovering depth from camera images by comparing two or more views of the same scene. The eyes catch two separate perspectives of a three-dimensional object in stereo vision. The parallaxes of retinal pictures are transformed into depth perception in the brain, providing a 3D representation of the object in the consciousness of observers. Binocular stereo is a straightforward stereo vision technique that employs only two images, which are typically captured with parallel cameras separated by a horizontal distance known as the baseline [1]. The human eye is the perfect binocular stereo imaging system, and simulating the vision of the human eye to perceive surrounding objects is the eternal goal of binocular stereo vision technology. Stereo vision technology is preferred because of its benefits of being non-contact and full field and having low cost, high precision, and superior automation [2–4]. As technology advances, binocular stereo vision imaging systems are increasingly applied in various fields such as robot vision [4], spacecraft pose estimation [5], 3D measurements [6], 3D computer stereo vision, virtual reality (VR) [7], industrial inspection [8], etc.

The key to a binocular stereo vision imaging device is the binocular optical system, which typically consists of two lenses

and two sensors [1,9]. However, due to the different sensitivities of the two sensors, the dual-lens dual-sensor system needs extensive optical position adjustment of the two lenses as well as image processing adjustments [10]. Furthermore, viewing stereo vision for a long period causes some viewers more discomfort than viewing 2D vision during an operation such as endoscopic surgery [11]. Therefore, a stereo vision camera with a single objective and single sensor for comfortable vision is desirable.

The binocular optical system has appeared in a variety of structure types with the development of binocular stereo vision. Design approaches of binocular optical systems have attracted a lot of attention from researchers. Kumar *et al.* [12] created a cooperative stereo system that can localize a moving target in a complex environment utilizing two pan-tilt-zoom (PTZ) cameras. Huang *et al.* [13] proposed a panoramic annular stereo imaging system based on the panoramic annular lens (PAL). The system contains two sets of PAL units placed coaxially and imaged on the same sensor; its imaging circle is two rings connected inside and outside, and the object is imaged in the two rings through the two PAL units. Guo *et al.* [8] proposed a new binocular optical system with a double objective and single sensor that realizes the 3D measurement function of industrial endoscopes, but due to the unreasonable layout of

the imaging position of the dual-channel optical system on a single detector, stray light is more severe when the optical lens is imaged. Recently, Canon announced a focal length of 5.2 mm, with a field of view of  $180^\circ$  for dual-objective single-sensor VR fisheye optics, which is not only compact but also separates two images imaged on the light-sensitive surface of the detector, thus better reducing stray light from the system [14]. Among these, the most widely used is the dual-camera imaging system. The measurement accuracy of the binocular camera is determined mainly by the focal length, principal point, distortion, and relative angle of the two optical axes of the cameras. Therefore, to ensure measurement accuracy, the internal orientation elements of the binocular camera must be calibrated with high accuracy [10,15–18]. In addition, the relative position of the conventional binocular camera will change slightly as the service time increases, and this slight change will seriously affect the measurement accuracy of the binocular camera. Therefore, binocular cameras need to be calibrated periodically.

For the problems of conventional binocular cameras such as regular calibration, large size, and visual fatigue, this paper proposes a novel single-lens single-sensor binocular stereo vision optical system that uses a lens array to achieve a dual-frame and images two images simultaneously on a single sensor. The aperture stop of the optical system is located at the framing-lens position to avoid vignetting. The layout of the imaging positions of the dual-channel optical system is optimized, and a mechanical design method for stray light is provided to eliminate the overlap of the imaging locations of the dual-channel optical system on the sensing surface of the sensor. Finally, a single-lens binocular optical system is created to demonstrate the feasibility of the concept.

## 2. DESIGN PRINCIPLE OF STEREO VISION OPTICAL SYSTEM

### A. Comparison and Selection of Stereo Vision Systems

Currently, there are three main conventional frame-based binocular stereo vision imaging technologies: single-lens scanning stereo imaging technology, dual-objective dual-sensor stereo imaging technology, and dual-objective single-sensor stereo imaging technology [19,20].

Single-lens scanning stereo imaging technology uses one camera to image the object, i.e., the first image, and then rotates or shifts the camera for the second image, forming two images of the object from different viewpoints, and finally to obtain the 3D information of the object through image processing. The advantages of this method are high image resolution, small size, and lightweight equipment, and it is widely used for long-range ranging. The disadvantage is that the target must remain stationary for a long time, and a precise motion control mechanism is required to control the precise baseline distance to ensure that the obtained stereo information meets the requirement of low error. Also, the method cannot meet the demand for real-time stereo imaging.

The dual-objective dual-sensor stereo imaging principle is illustrated in Fig. 1. The relative positions of camera 1 and camera 2 are fixed, and they are fixed together on a slider. The

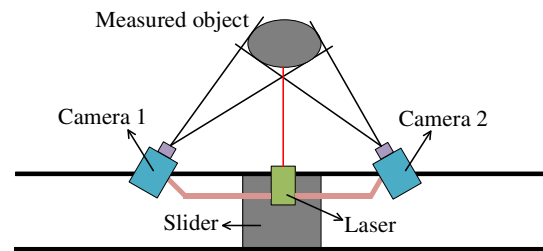


Fig. 1. Dual-objective dual-sensor imaging system.

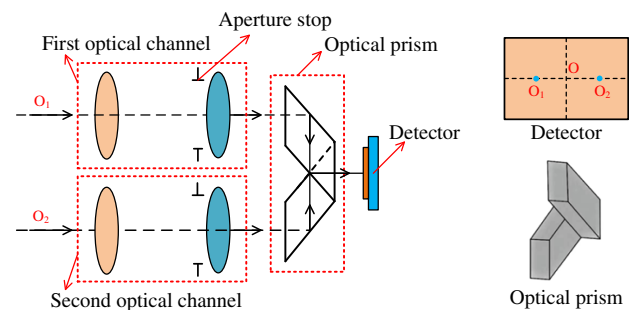


Fig. 2. Imaging principle diagram of the dual-objective single-sensor optical system.

slider is used to drive the binocular cameras to move for measuring different objects. This stereo imaging method can obtain the 3D information of the object under test in real time, but the internal parameters and relative positions of cameras 1 and 2 must remain unchanged after calibration, so the system must be calibrated periodically to guarantee the accuracy of the 3D information of the object under test. The advantages of this imaging method are good real-time stereo information acquisition, the ability to record dynamic images, no motion mechanism, and high reliability. The disadvantages are the large size of the equipment and high cost. In addition, the accuracy of the obtained stereo information is not very high because of possible individual errors from the two lenses, which are generally used in low-precision stereo vision acquisition systems.

Dual-objective single-sensor stereo imaging technology was created to reduce the size of the entire system while also addressing the issue of periodic calibration. Figure 2 illustrates the principle of dual-objective single-sensor stereo imaging [8]. To convert the images of the two optical channels onto one detector and ensure that the left and right images on the image sensor do not conflict with each other, the system uses two  $45^\circ$  angled rhomboid prisms that intersect  $180^\circ$ . To make sure that the emitting surfaces of the two prisms are common planar, they are glued together side by side.

Compared to the two previously mentioned techniques, the dual-objective single-sensor stereo imaging method gives incomparable benefits, including real-time imaging, no secondary calibration, light weight, compact size, and low cost. However, this stereo imaging method uses two objectives for dual-frame imaging. This paper presents a single-objective single-sensor stereo imaging optical system design approach to avoid the requirement of two objectives and visual fatigue.

## B. Design Principle of Single-Sensor-Based Binocular Stereo Vision Optical System

The single-sensor-based binocular optical system uses a lens array for beam splitting, which consists mainly of a front lens group, framing lenses, and a compensation lens group, and its imaging principle is shown in Fig. 3. To avoid vignetting of the two optical channels, the optical system of the two channels shares a front lens group, and the framing lens is set at the aperture stop of the optical system. The framing lens array is made up of two identical small lenses,  $A_1$  and  $A_2$ , which are symmetric about the  $xoz$  plane. Since the two frame lenses are symmetrical, a complete single-objective binocular optical system through symmetry. The use of a frame lens results in a non-axisymmetric single-channel optical system, and the aberration of the optical system is bound to change significantly after the off-axis design of the frame lens. As a result, after the dual-frame lens array, a compensation lens group is introduced to better correct the aberration of the off-axis optical system and improve imaging quality. The compensation lens group compensates for the aberration of the two single-channel optical systems simultaneously, which has rotational symmetry.

To better solve the problem of overlapping and stray light interference in dual-channel imaging images, this paper proposes a joint optimized design for the structural parameters of the framing lens and the imaging area division of the detector. The distribution of the imaging positions of the two channels on the single sensor is shown in Fig. 4.  $O$  is the center of the detector, and  $O_1$  and  $O_2$  are the imaging positions at the center field of view of the first and second channels, respectively, where  $O_1$  and  $O_2$  are symmetric about point  $O$ . The length and width of the detector's sensing surface are shown in Fig. 4. To avoid overlapping imaging positions of the two channels on the detector, the imaging position on the long side direction of the detector is set to  $h$  at the edge field of view of the dual channel, while the imaging height is set to  $r$  for the single-channel optical system. The imaging position of the center field of view of the dual-channel optical system is the distance from the center of the detector to  $h/2 + r$ . To assure that the detector can receive the full field of view image, the following equation must be satisfied:

$$L \geq h + 4r, \quad (1)$$

where  $L$  is the longer side of the detector.

When designing an optical system, the imaging height of the system must normally be greater than half the diagonal length of the detector; however, in this paper, the opposite is true. Therefore, the effect of light greater than the edge field of view on the normal imaging area of the adjacent channel must be considered after imaging the optical system. The difference between the imaging height of the optical system with zero

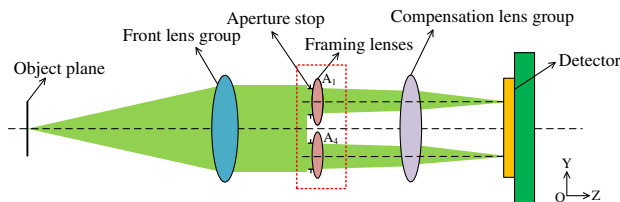


**Fig. 3.** Imaging schematic of a single-sensor-based binocular stereo vision optical system.

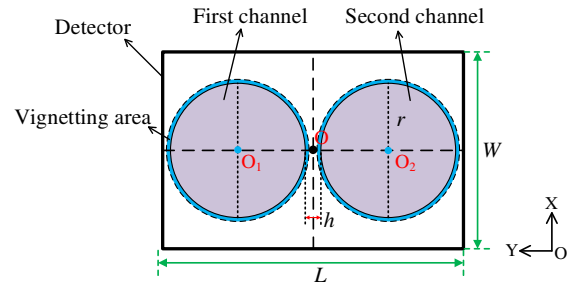


**Fig. 4.** Imaging position layout of the binocular optical system.

illumination and the imaging height of the fringe field of view is  $\Delta h$ . To avoid the influence of stray light on the normal imaging area, the equation needs to be satisfied as

$$h \geq 2\Delta h. \quad (2)$$

At this point, the binocular optical system's maximum field of view is

$$\theta = \arctan \left( \frac{L - h}{4f} \right), \quad (3)$$

where  $f$  is the focal length of the binocular optical system.

The framing lens  $A_1$  will be translated along the  $y$ -axis direction to move the imaging point of the central field of view of the first channel from point  $O$  to point  $O_1$ , as shown in Figs. 3 and 4. To move the imaging point of the central field of view of the first channel from point  $O$  to point  $O_1$ , the translation distance  $s$  must satisfy the following relationship as

$$s = k \times \left( \frac{h}{2} + r \right), \quad (4)$$

where  $k$  is the displacement coefficient of the framing lens, and the magnitude of this coefficient is related to the off-axis aberration correction of the compensation lens group.

The detector utilization  $\eta$  is the ratio of the imaging area of the two optical channels on the detector light-sensitive surface to the detector light-sensitive surface area:

$$\eta = \frac{S_1 + S_2}{S} \times 100\% = \frac{2\pi r^2}{LW} \times 100\%, \quad (5)$$

where  $S_1$  and  $S_2$  denote the imaging area of the first optical channel and second optical channel on the detector sensing surface, respectively, and  $S$  denotes the area of the detector sensing surface.

In the process of designing a binocular optical system, first it is necessary to follow the coaxial optical system, then move the framing lens along the  $y$ -axis direction by a distance  $s$ , put the optical stop on the framing-lens position, and then carry out further optimization to realize beam splitting. It is also necessary to ensure that there is sufficient mechanical mounting space between binning lenses  $A_1$  and  $A_2$  during the optical system binning process. To improve imaging quality and better correct the aberration of the off-axis optical system, a compensation lens group is added after the framing lens array, and the compensation lens group compensates for the aberration of the two single-channel optical systems simultaneously.



### 3. BINOCULAR STEREO VISION OPTICAL SYSTEM DESIGN

#### A. Design Specifications

Considering the desire to improve the spatial resolution of the binocular stereo imaging system, a half-frame detector with a sensor surface size of  $23.7 \text{ mm} \times 15.6 \text{ mm}$  is selected in this paper. The larger the field of view of the binocular stereo vision optical system based on a single sensor, the more difficult it is to correct the off-axis aberration. Nevertheless, to satisfy more application scenarios, the field of view of the stereo imaging optical system cannot be too small. Considering the size of the field of view of the optical system and the design difficulty, the design in this paper requires a full field of view of  $30^\circ$ . To avoid the overlap of the two imaging images and to better lay out the stray light mechanical structure, the imaging interval between the two images is greater than  $0.5 \text{ mm}$ . The overall design specification of the single-sensor-based binocular stereo vision optical system is presented in Table 1.

#### B. Single-Lens Single-Sensor Binocular Stereo Vision Optical System Design

The optical system example design is implemented using the design method of a binocular stereo vision optical system based on a single sensor, as proposed in this paper. The coaxial optical system is first designed according to the design specifications in Table 1, then the optical stop and the framing lenses are moved together along the  $y$ -axis direction to perform dual-channel design of the coaxial optical system. In the process of dual-channel design, it is necessary to ensure that there is enough mechanical mounting space between the framing lenses. Through the above steps, the optical system after the dual-channel off-axis design is illustrated in Fig. 5. The total length of the binocular optical system is  $78 \text{ mm}$ . However, due to the large off-axis aberration, the imaging quality of the dual-channel optical system is poor.

Focusing on improving the imaging quality of the non-axisymmetric optical system after the dual-channel off-axis design, and employing the off-axis aberration correction method proposed in this paper, the compensation lens group is added after the framing lenses. After the overall optimization design, the focal distance distribution of each group of the binocular stereo vision optical system is shown in Table 2.

The structure of the finally designed binocular optical system is illustrated in Fig. 6. The binocular optical system uses two identical single lenses for beam splitting, with the aperture stop

**Table 1. Design Specifications for Single-Sensor-Based Binocular Stereo Vision Optical System**

Parameters	Values
Working spectrum	480–660 nm
Effective focal length	20 mm
$F$ -number	4
Full field of view	$30^\circ$
Distortion	$\leq 2.5\%$
MTF (at 50 lp/mm)	$\geq 0.40$
Position interval $h$	$\geq 0.5 \text{ mm}$

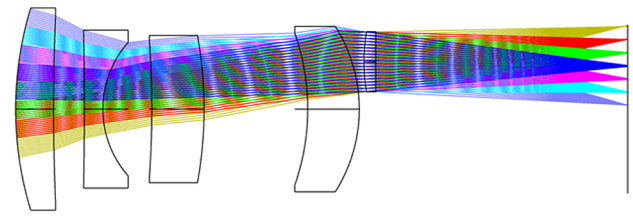
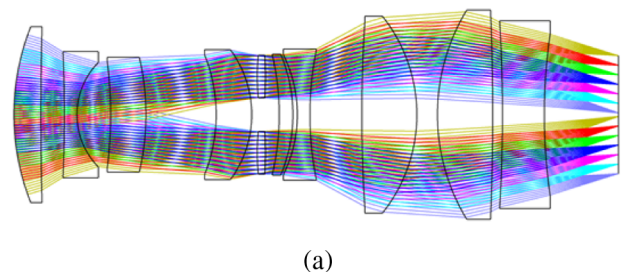


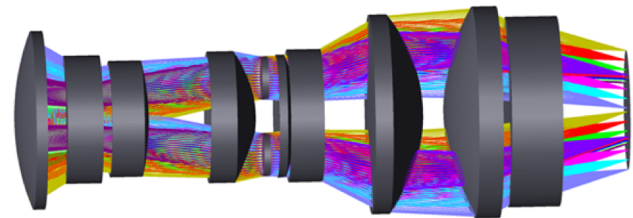
**Fig. 5.** Single-sensor-based binocular stereo vision optical system layout.

**Table 2. Focal Length of Each Group**

Groups	Front Lens Group	Framing Lens	Compensation Lens Group
Focal length	178.2 mm	39.6 mm	40.5 mm



(a)



(b)

**Fig. 6.** Single-sensor-based binocular stereo vision optical system layout. (a) 2D layout and (b) 3D layout.

located on the front surface of the framing lens; the distance between the upper and lower edges of the two framing lenses is  $6 \text{ mm}$ , leaving enough space for lens assembly. The total length of the binocular optical system is  $110 \text{ mm}$ , and the maximum aperture of the lens is  $40 \text{ mm}$ .

#### C. Image Quality Evaluation

The vital evaluated indices of optical system image quality evaluation include mainly the modulation transfer function (MTF), spot diagram, and grid distortion. The MTF can reflect the imaging quality of the optical system more comprehensively, and generally speaking, the higher the MTF, the better the imaging quality of the optical system. The average MTF (seen in Fig. 7) value of the full field of view at  $50 \text{ lp/mm}$  is greater than  $0.4$ , which indicates the system has good imaging quality.

After an object point is imaged by the optical system, the spot diagram can reflect the imaging spot diffusion on the image plane; the smaller the imaging spot, the better the imaging quality of the optical system. The imaging spot diagram of a



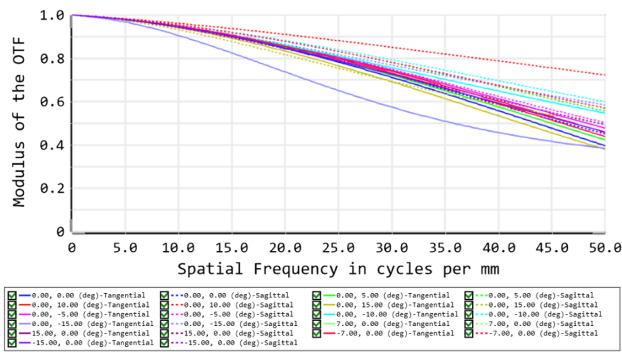


Fig. 7. Modulation transfer function curve.

single-sensor-based binocular stereo vision optical system is illustrated in Fig. 8, which further reveals the good imaging quality.

The single-sensor binocular stereo vision optical system is a non-axisymmetric optical system, so the aberrations of the optical system are asymmetric about the central field of view. To evaluate the aberrations of the full field of view of the optical system more comprehensively, it is necessary to use the grid aberrations for evaluation. The design results indicate that the maximum distortion of the system is less than 2.2% in the full field of view.

#### D. Tolerance Analysis

Tolerance analysis is one of the important analysis aspects before optical lens manufacturing and a key part of determining the success or failure of optical system design. Using the tolerance

Table 3. Tolerance Distribution of Binocular Optical Systems

Tolerance Items	Value
Radius (fringe)	$\leq 3$
Thickness (mm)	$\pm 0.03$
Surface decenter (mm)	$\pm 0.02$
Element tilt ( $^{\circ}$ )	$\pm 0.02$
Element decenter (mm)	$\pm 0.02$
Surface irregularity (fringe)	$\leq 0.3$
Refractive index	$\pm 0.005$
Abbe number (%)	$\pm 0.5$

analysis function in the optical design software Zemax, the manufacturing difficulty of the lens can be easily evaluated. After the tolerance sensitivity analysis, the tolerance distribution of the single-lens binocular optical system is presented in Table 3. After Monte Carlo analysis, the average MTF distribution curve (shown in Fig. 9) of the full field of view of the binocular optical system indicates that 80% of the systems in the Monte Carlo simulation have an average MTF greater than 0.29 at 50 lp/mm. The above tolerance analysis demonstrates the good manufacturing feasibility of this optical system.

#### 4. IMAGING POSITION SIMULATION AND STRUCTURE DESIGN

To more clearly and intuitively understand the imaging principle of parallax generation of a single-objective single-sensor binocular stereo vision optical system, the optical path diagram (seen in Fig. 10) of the field of view generation is given. The

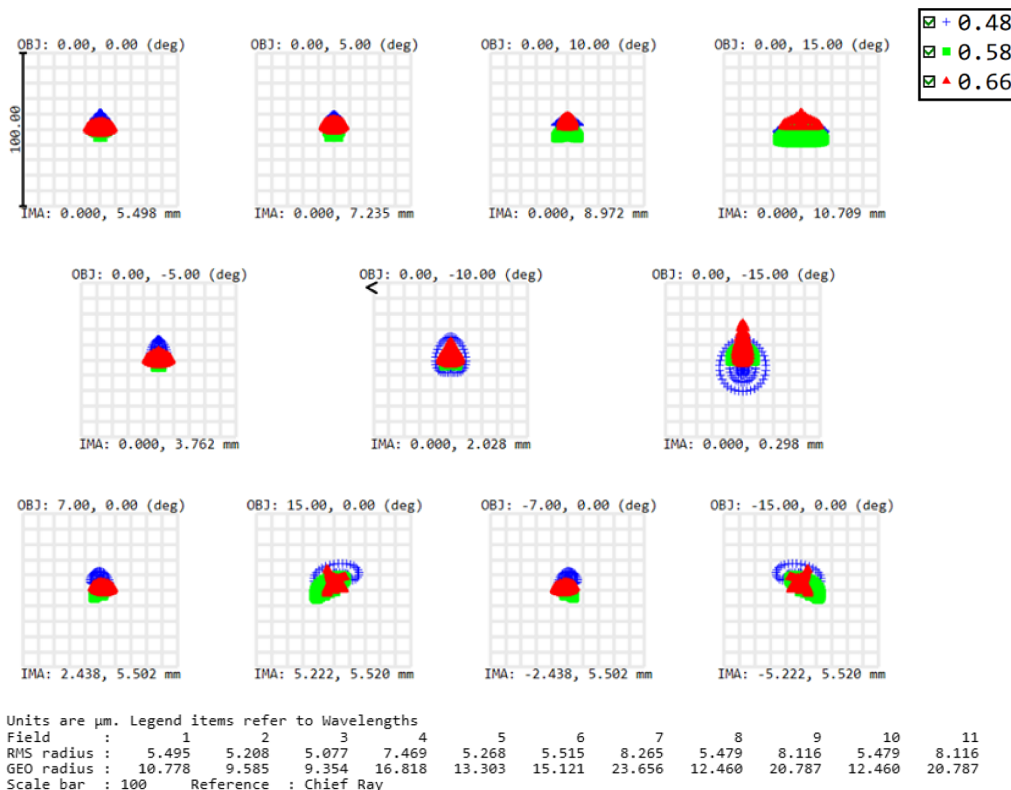
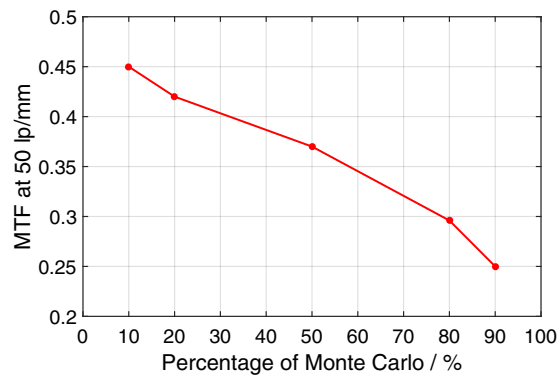
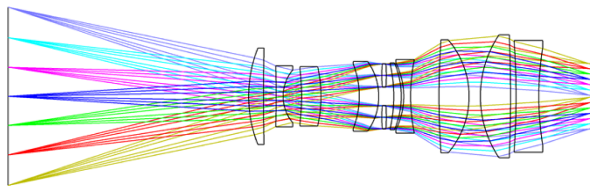


Fig. 8. Spot diagram of the single-sensor-based binocular stereo vision optical system.



**Fig. 9.** Monte Carlo analysis diagram.



**Fig. 10.** Parallax optical path diagram of the binocular optical system.

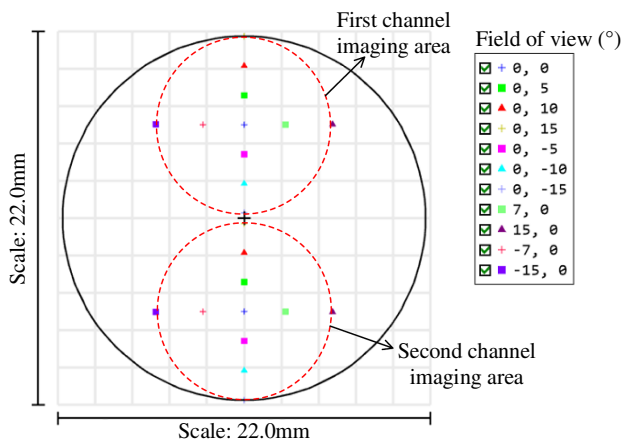


**Fig. 11.** Distribution of imaging positions in the image plane.

binocular optical system for the same object point imaging produces a certain angle parallax, and the farther the object distance, the smaller the imaging angle parallax. Parallax generation provides a strong guarantee for the acquisition of 3D stereo images.

The simulated imaging positions of the two channels of the binocular optical system in the focal plane and the imaging positions of each field of view are depicted in Fig. 11. The imaging area of the single-channel optical system is circular, and the circumferential diameter of the two circular imaging areas is 22 mm.

The stray light outside the field of view of the two-channel optical system will be imaged in the normal imaging area of the adjacent channel optical system, thus reducing the imaging quality of the optical system, so this paper proposes the use of a baffle to eliminate the cross talk problem of stray light from the adjacent channel. After designing the baffle at the back

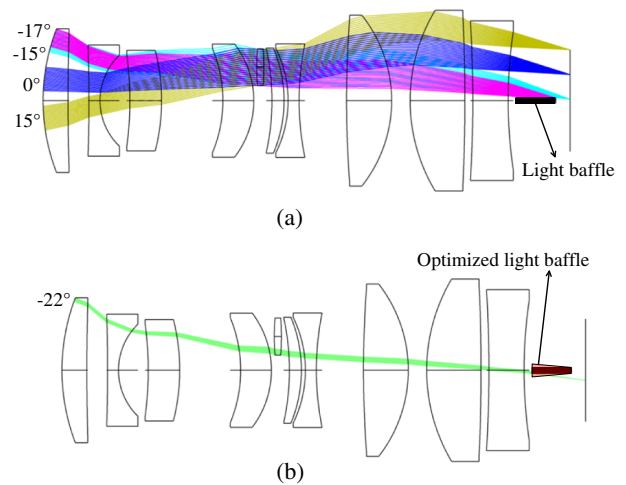


**Fig. 12.** Stray light path diagram outside the field of view. (a) Stray light path diagram with a field of view of  $-17^\circ$  and (b) stray light path diagram with a field of view of  $-22^\circ$ .

intercept of the two-channel optical system, the propagation path of stray light outside the field of view is shown in Fig. 12. From Fig. 12(a), the stray light at the field of view of  $-17^\circ$  is just blocked by the baffle, and the baffle has no effect on the imaging beam at the  $-15^\circ$  edge of the field of view. When using the original structure size baffle, it can be seen from Fig. 12(b) that a small part of stray light from the  $-22^\circ$  field of view enters the optical system. When an optimized baffle is utilized, stray light can no longer enter the imaging system. Consequently, light with a field of view greater than  $22^\circ$  does not affect the imaging quality of the adjacent channel optical system. The above analysis suggests that a reasonably designed baffle structure can effectively solve the cross talk problem of stray light in the two-channel optical system.

The simulation analysis of the two-channel optical system reveals that when the object distance is infinite, the back intercept distance is 13.491 mm and the distance between the two images is 0.594 mm. When the object distance is 2 m, the back intercept distance is 13.676 mm and the distance between the two images is 0.598 mm. In other words, when the object distance changes, the imaging position of the two images hardly changes. Only the baffle and the imaging surface change by 0.185 mm. Therefore, the imaging area with a length of 0.185 mm is disturbed by stray light, when the detector and the baffle can be made into a single unit. When focusing, the detector and the light baffle move together to eliminate stray light interference in the imaging area. At this point, the distance to the imaging object of the optical system may be less than 2 m.

Following the optimized design method of the mechanical structure for stray light elimination in Fig. 12, the 3D mechanical structure of the single-sensor-based binocular stereo vision imaging lens can be designed. In the rear section of the lens, a very critical light baffle is designed to eliminate stray light, while ensuring that the light baffle and the detector are a whole to avoid stray light when the optical system is focusing.

## 5. CONCLUSION

This paper proposes a novel design method for a single-lens, single-sensor binocular stereo vision optical system. The method uses two small lenses symmetrical about the optical axis to screen the imaging light to achieve a dual frame, and the images of two channels are simultaneously imaged on different areas of one detector by reasonable structural parameter matching. The system is made more compact by using two optical channels with a common front lens group and a compensation lens group. Finally, a single-lens binocular optical system with a focal length of 20 mm and an  $f$ -number of four is designed. The design method proposed in this paper provides a new design idea for the development of a single-sensor binocular stereo vision camera; it makes up for the defects of a traditional binocular stereo camera with high development cost and difficult calibration, and has wide application prospects in the fields of robot vision and VR.

**Funding.** Instrument Development of Chinese Academy of Sciences (YJKYYQ20200060); Sichuan Science and Technology Program (2022YFG0249, 2022103, 2021JDRC0084).

**Disclosures.** The authors declare no conflicts of interest.

**Data availability.** Data underlying the results presented in this paper are not publicly available at this time but may be obtained from the authors upon reasonable request.

## REFERENCES

1. H. Rosas, *Reality and Perception in Stereo Vision: Technological Applications* (InTech, 2011).
2. Q. Wu, X. Wang, L. Hua, and G. Wei, "The real-time vision measurement of multi-information of the bridge crane's workspace and its application," *Measurement* **151**, 107207 (2019).
3. K. T. Song and J. C. Tai, "Dynamic calibration of pan-tilt-zoom cameras for traffic monitoring," *IEEE Trans. Syst. Man Cybern. B, Cybern.* **36**, 1091–1103 (2006).
4. O. Sergiyenko, "Optoelectronic system for mobile robot navigation," *Optoelectron. Instrum. Data Process.* **46**, 414–428 (2011).
5. L. Zhang, F. Zhu, Y. Hao, and W. Pan, "Optimization-based non-cooperative spacecraft pose estimation using stereo cameras during proximity operations," *Appl. Opt.* **56**, 4522–4531 (2017).
6. P. Zhao and N. H. Wang, "Precise perimeter measurement for 3D object with a binocular stereo vision measurement system," *Optik* **121**, 953–957 (2010).
7. L. Christodoulou, "Overview: 3D stereo vision camera-sensors-systems, advancements, and technologies," in *3D Stereo Vision Camera-sensors, Advancements, and Technologies* (Cyprus University of Technology, 2013), p. 73.
8. J. F. Guo, P. Liu, G. H. Jiao, Y. F. Lu, and J. C. Lü, "Binocular optical system of industrial endoscope for three-dimensional measurement," *Opt. Precis. Eng.* **22**, 2337–2344 (2014).
9. K. Kroeker, "Looking beyond stereoscopic 3D's revival," *Commun. ACM* **53**, 14–16 (2010).
10. R. Tsai, "A versatile camera calibration technique for high-accuracy 3D machine vision metrology using off-the-shelf TV cameras and lenses," *IEEE J. Rob. Autom.* **3**, 323–344 (1987).
11. M. Lambooi, W. Ijsselstein, M. Fortuin, and I. Heynderickx, "Visual discomfort and visual fatigue of stereoscopic displays: a review," *J. Imaging Sci. Technol.* **53**, 030201 (2009).
12. S. Kumar, C. Micheloni, and C. Piciarelli, "Stereo localization using dual PTZ cameras," in *Computer Analysis of Images and Patterns (CAIP)* (2009).
13. Z. Huang, J. Bai, and X. Hou, "Design of panoramic stereo imaging with single optical system," *Opt. Express* **20**, 6085–6096 (2012).
14. "Canon RF 5.2mm F/2.8L dual fisheye 3D VR lens announced," <https://www.cined.com/canon-rf-5-2mm-f-2-8l-dual-fisheye-3d-vr-lens-announced>.
15. D. Wan and J. Zhou, "Stereo vision using two PTZ cameras," *Comput. Vis. Image Underst.* **112**, 184–194 (2008).
16. Y. Cui, F. Zhou, Y. Wang, L. Liu, and H. Gao, "Precise calibration of binocular vision system used for vision measurement," *Opt. Express* **22**, 9134–9149 (2014).
17. T. Jiang, X. Cheng, and H. Cui, "Calibration method for binocular vision with large FOV based on normalized 1D homography," *Optik* **202**, 163556 (2020).
18. H. Zhu, M. Wang, and W. Xu, "Research on calibration method of binocular vision system based on neural network," *Secur. Commun. Netw.* **2021**, 5542993 (2021).
19. G. Y. Belay, H. Ottevaere, Y. Meuret, M. Vervaeke, J. Van Erps, and H. Thienpont, "Demonstration of a multi-channel, multiresolution imaging system," *Appl. Opt.* **52**, 6081–6089 (2013).
20. L. Smeesters, G. Y. Belay, H. Ottevaere, Y. Meuret, M. Vervaeke, J. V. Erps, and H. Thienpont, "Two-channel multiresolution refocusing imaging system using a tunable liquid lens," *Appl. Opt.* **53**, 4002–4010 (2014).